MeCP2 binding to DNA depends upon hydration at methyl-CpG

Molecular Cell
Short Article

MeCP2 Binding to DNA Depends upon Hydration at Methyl-CpG

Kok Lian Ho,[1] Iain W. McNae,[1] Lars Schmiedeberg,[1] Robert J. Klose,[1,2] Adrian P. Bird,[1,*] and Malcolm D. Walkinshaw[1,*]
[1]School of Biological Sciences, University of Edinburgh, King's Buildings, Mayfield Road, Edinburgh EH9 3JR, UK
[2]Present address: Department of Biochemistry, Oxford University, South Parks Road, Oxford OX1 3QU, UK.
*Correspondence: m.walkinshaw@ed.ac.uk (M.D.W.), a.bird@ed.ac.uk (A.P.B.)
DOI 10.1016/j.molcel.2007.12.028

SUMMARY

MeCP2 is an essential transcriptional repressor that mediates gene silencing through binding to methylated DNA. Binding specificity has been thought to depend on hydrophobic interactions between cytosine methyl groups and a hydrophobic patch within the methyl-CpG-binding domain (MBD). X-ray analysis of a methylated DNA-MBD cocrystal reveals, however, that the methyl groups make contact with a predominantly hydrophilic surface that includes tightly bound water molecules. This suggests that MeCP2 recognizes hydration of the major groove of methylated DNA rather than cytosine methylation per se. The MeCP2-DNA complex also identifies a unique structural role for T158, the residue most commonly mutated in Rett syndrome.

INTRODUCTION

DNA methylation is an epigenetic signal in mammalian cells that affects gene regulation, genomic stability, and chromatin structure (Bird, 2002). The signal can be interpreted by a family of proteins that recognize symmetrically methylated 5′CpG3′ (mCpG) pairs via a methyl-CpG-binding domain (MBD) (Hendrich and Bird, 1998; Nan et al., 1993). Three family members (MeCP2, MBD1, and MBD2) are able to recruit corepressor complexes that can inhibit transcription with the aid of chromatin-modifying enzymes. This study concerns the molecular basis of the DNA-binding specificity of the transcriptional repressor MeCP2 (Jones et al., 1998; Nan et al., 1997, 1998). Mutations within the human *MECP2* gene are responsible for 95% of cases of the autism spectrum disorder Rett syndrome (RTT) and are also implicated in X-linked mental retardation and several other neurological conditions (Amir et al., 2000; Neul and Zoghbi, 2004). Studies of mice lacking MeCP2, which are convincing models of RTT, have implicated MeCP2 in synaptogenesis and in the maintenance of neuronal function (Bienvenu and Chelly, 2006). Restoration of the protein in MeCP2-deficient mice with advanced neurological symptoms leads to reversal of many aspects of the phenotype, suggesting that RTT may also be therapeutically reversible in humans (Guy et al., 2007).

Solution structures of unliganded MBDs of MBD1 (Ohki et al., 1999) and MeCP2 (Wakefield et al., 1999) and of a DNA-bound MBD of MBD1 (Ohki et al., 2001) have been established by NMR. Based on the structure of the MBD1-DNA complex, it was inferred that the specificity for methylated DNA was due to contacts between a hydrophobic patch on the MBD that interacts with the DNA methyl groups directly. In this structural study, we focused on the MBD itself, as over half of the missense mutations in RTT patients are localized to this domain. Previous studies have tested the effects of RTT mutations on DNA binding and established that the majority of those within the MBD reduce the affinity for methylated DNA (Ballestar et al., 2000; Free et al., 2001; Kudo et al., 2001). The X-ray structure of the MeCP2 MBD complex presented here rationalizes the effects of the most common Rett mutations and provides a general model for methylated DNA binding that is dependent on structured waters.

RESULTS AND DISCUSSION

To obtain a high-resolution crystal structure of the MeCP2 MBD-DNA complex, we took account of recent evidence that a run of four or more AT bases adjacent to the symmetrical mCpG dinucleotides promotes high-affinity binding of MeCP2 (Klose et al., 2005). A polypeptide corresponding to amino acids 77–167 of the MeCP2 MBD domain (Figure 1) was expressed and cocrystallized with a 20 bp DNA fragment of promoter III (nucleotides −108 to −90) of the mouse-brain-derived neurotrophic factor (*BDNF*) gene, which contains a central mCpG pair and an AT run. This promoter (Figure 2A) is implicated as an MeCP2 target (Chen et al., 2003; Martinowich et al., 2003).

Crystals of a selenomethionine form of MeCP2-MBD (A140SeMet, SeMet94) were used to provide sufficient anomalous signal for phase determination using SAD (Table 1). Soaking the crystals in $MnCl_2$ solution improved resolution from 3 to 2.5 Å. Crystals of the wild-type protein (A140) had an essentially identical structure with a C_α rmsd fit of 0.44 Å (Table 1). The structure of the MeCP2-MBD in complex with DNA (Figure 2B) is similar to that of the unliganded structure determined by NMR (Wakefield et al., 1999), with an rmsd fit for C_α atoms of 2.33 Å (Figure 2C). The most notable difference concerns loop L1, which is drawn toward the DNA through four hydrogen bonds with the phosphate backbone on the face of the major groove that includes the pair of cytosine methyl groups (Figure S1).

The mCpG-binding surface is unexpectedly hydrophilic. The C5 methyl groups (m5C8 and m5C33) form close contacts (<4 Å) with 13 and 12 neighboring atoms, respectively (Figure 2D and see Table S1 available online). Of these 25 interactions, only

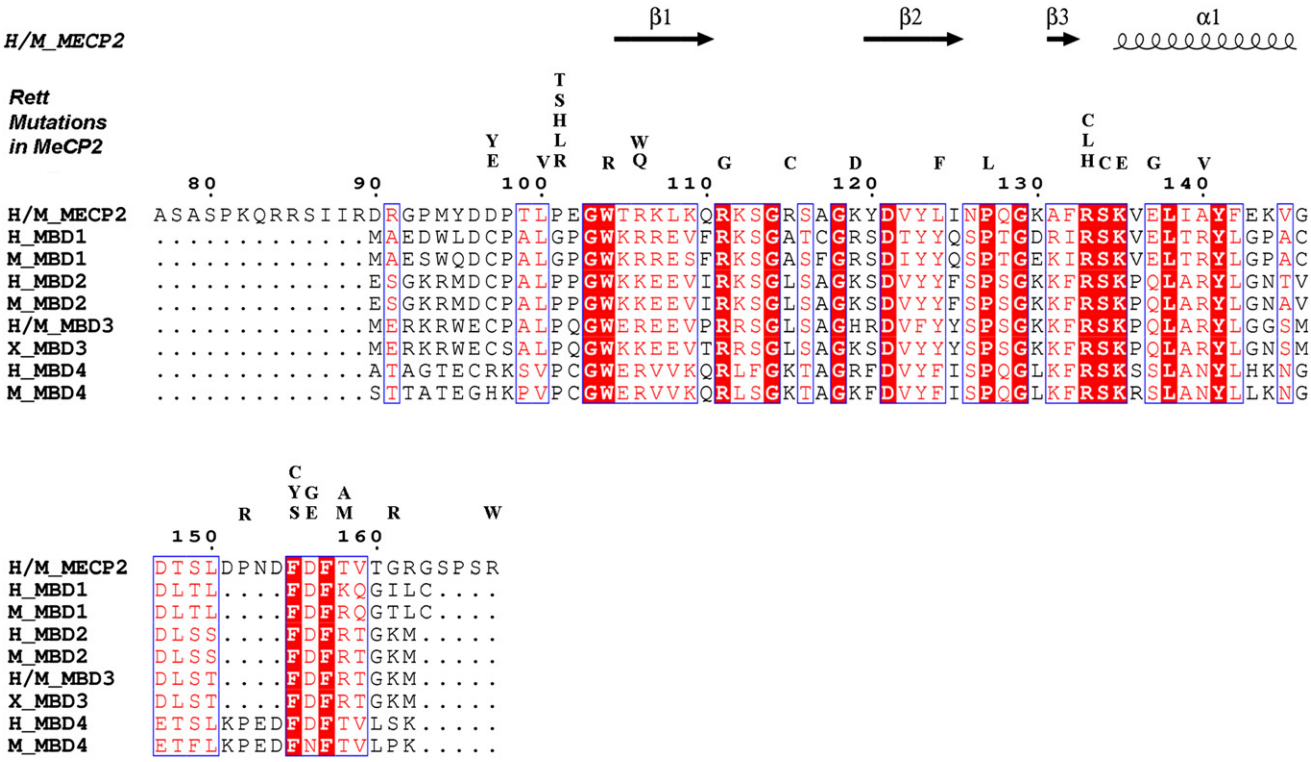

Figure 1. Sequence Comparison of Methyl-CpG-Binding Domains of the MBD Protein Family from Human, Mouse, and *Xenopus*

Secondary structure elements from the X-ray structure of MeCP2 are denoted by arrows (β strand) and coils (α helix). Mutations that have been associated with neurological disease are shown. Human (H), mouse (M), and *Xenopus* (X).

two (m5C33 to R133CG and R133CB) are classically hydrophobic in character. MeCP2 recognition of mCpG involves the five water molecules W12, W24, W10, W21, and W22, each making a CH…O interaction (Figure 2). W24 and W22 form a tetrahedral arrangement of hydrogen bonds that bridge DNA with protein and also make CH…O interactions with both methyl groups of the mCpG dinucleotide pair (Figures 2D and 2E). W22 forms four hydrogen bonds with D121, W24, W21, and N4 of m5C33 plus a CH…O interaction with the C5 methyl group of m5C33. W24 forms four conventional hydrogen bonds with Y123, R133, W22, and N4 of m5C8 plus a CH…O interaction with the methyl group of m5C8 (Figures 2D and 2E and Table S1). Interestingly, CH…O hydrogen bonds have been implicated in methyl group recognition during lysine methylation by SET domain lysine methyltransferases (Couture et al., 2006).

The only MeCP2-MBD residues that directly interact with DNA bases in the crystallized *BDNF* sequence are D121, R111, and R133 (Figures 2D and 2E and Table S1). D121 makes a CH…O hydrogen bond of 3.5 Å with the methyl group of m5C8 (Figure 2D). The hydrogen bonds formed between the symmetrical arginine fingers (R111 and R133) and each guanine of the mCpG pair (Figure 2E) occur frequently in diverse examples of protein-DNA recognition (Luscombe et al., 2001). Both arginine fingers lie in a plane with the guanine bases and are locked in position by salt bridges with the carboxylates of D121 and E137 (Table S1). This symmetrical arrangement of the arginine side chains places the guanidinum groups directly above/beneath the methyl groups of the methylated cytidine bases with an average methylguanidinium distance of 3.7 Å (Figure 2D). Specificity for the mCpG base pair derives in part from the constrained configuration of arginine side chains in contact with the juxtaposed guanines that are exclusive to the CpG sequence motif.

We considered the possibility that structurally conserved water molecules that are present due to cytosine methylation in the major groove determine the mCpG-binding specificity of MeCP2. There are currently 47 m5C-containing double-stranded DNA structures in the Nucleic Acid Database with a resolution better than 3 Å (Berman et al., 1992). Of these, 78% have at least one m5C base coordinating a water molecule through a CH…O hydrogen bond to the methyl carbon and simultaneously a conventional hydrogen bond to N4 (similar to the interactions shown by W22 and W24). Additionally, 84% contain at least one water molecule bridging a DNA phosphate group to the methyl group of m5C (similar to the interactions shown by W12 and W10). This methylation-specific hydration pattern has been noted previously and was speculated to potentially specify recognition of methylated DNA by proteins (Mayer-Jung et al., 1998).

The importance of water in MBD recognition is supported by mutagenesis studies of MBDs from MeCP2 and MBD1. Y123 is of particular interest, as its contact to DNA is via two bridging hydrogen bonds from its hydroxyl group to W24 and W12 (Figure 2E). The Y123F mutant lacks this hydroxyl group and has a reduced affinity for methylated DNA (Figure 3). The loss of binding is therefore attributable solely to the interaction of the hydroxyl

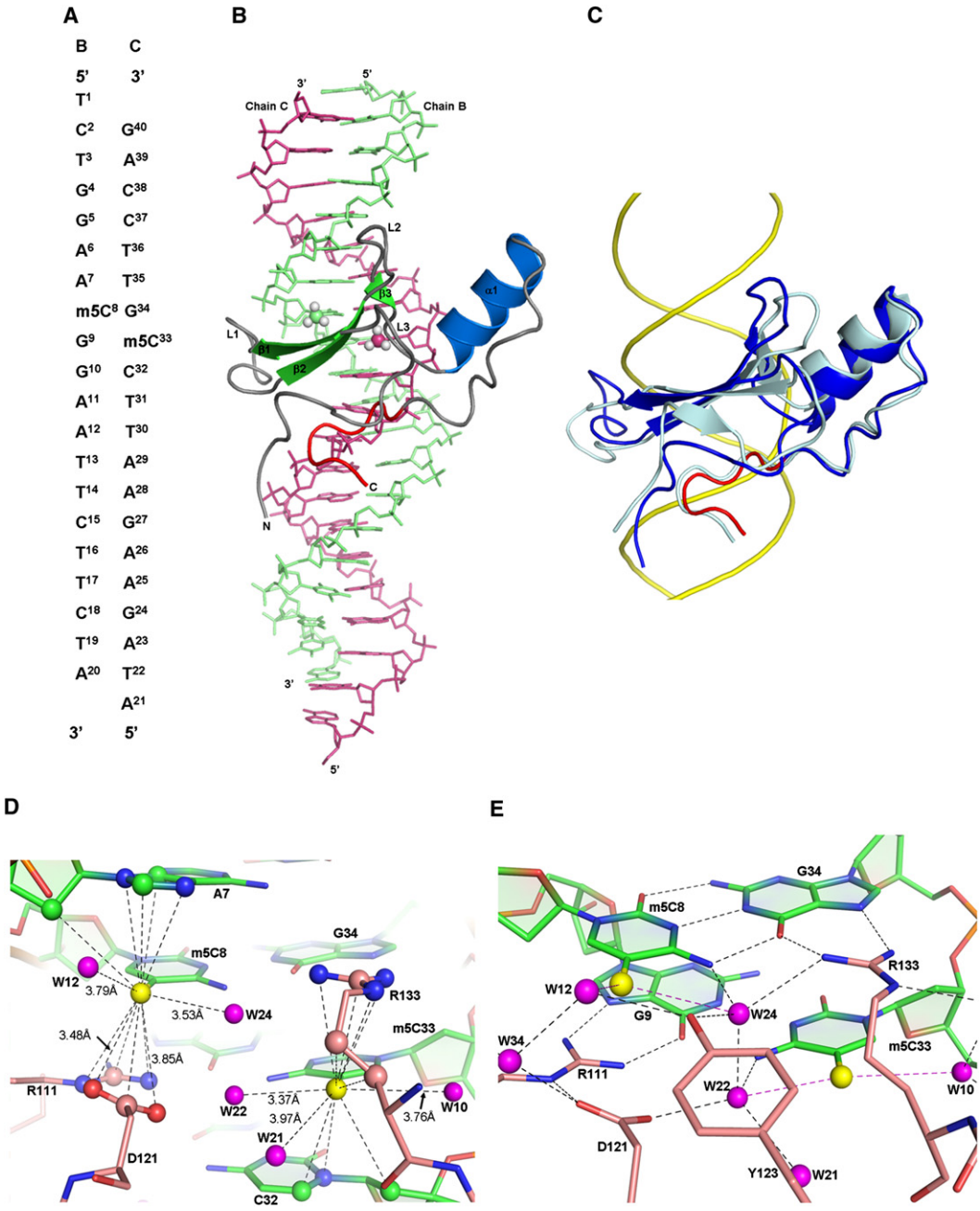

Figure 2. The X-Ray Structure of MeCP2-MBD Complexed with *BDNF* Promoter DNA at 2.5 Å

(A) *BDNF* promoter DNA sequence used in the cocrystal X-ray structure. The overhanging T/A bases were incorporated to promote crystallization through end-to-end DNA stacking.

(B) The X-ray structure of the MeCP2-MBD in complex with DNA. The methyl groups of the mCpG pair are shown as spheres. The β strands (green) and α helix (blue) are connected by the loops L1 (R111– K119), L2 (N126–K130), and L3 (R133–S134). The tandem Asx-ST motif (D156–R162) is highlighted in red.

(C) Overlay of the unliganded MeCP2 structure determined by NMR (gray) with the X-ray structure (blue and red) in complex with DNA (yellow). The Asx-ST-motif of the X-ray structure is highlighted in red.

(D) Nonbonded contacts to the m5C methyl groups. Black dashed lines show all nonbonded contacts to the m5C methyl groups of less than 4 Å. The m5C methyl groups are shown as yellow balls and water molecules W21, W22, and W24 as purple balls. Distances for all seven m5C methyl CH…O contacts are shown. A complete list of distances for these interactions is given in Table S1.

(E) Hydrogen-bonding interactions involving the mCpG pair. Hydrogen bonds are shown as black dashed lines. The two m5C methyl…water contacts are drawn as dashed red lines. Distances for all hydrogen bonds shown in this figure are tabulated in Table S2. Specific hydrogen bonds formed between R111 and G9 (chain B) and R133 and G34 (chain C) position the guanidinium groups directly over the methyl groups of the m5C bases.

Table 1. Crystallographic Statistics

Crystal	Selenium Peak (A140SeMet, SeMet94)	Native (A140)
Data Collection		
Space group	C2	C2
Unit cell lengths (Å)		
a	79.71	82.24
b	53.60	53.92
c	65.73	63.24
β (deg)	132.10	128.17
Wavelength (Å)	0.97800	0.97935
Outer resolution shell (Å)	2.64–2.50	2.85–2.70
Completeness (%)[a]	98.5 (90.7)	97.1 (87.3)
Anomalous completeness (%)[a]	98.4 (89.9)	—
Multiplicity[b]	7.1 (5.3)	3.5 (2.9)
Total reflections[a]	50,307 (5055)	20,686 (2157)
Unique reflections[a]	7122 (950)	5914 (750)
$<I>/\sigma(I)$[a]	19.7 (3.0)	13.5 (1.6)
R_{meas} (%)[c]	8.8 (47.4)	8.9 (62.5)
Refinement		
R_{cryst}[d]/R_{free} (%)	21.2/ 27.6	23.0/ 29.5
Geometry		
Rmsd bond/angles (Å, deg)	0.009/1.85	0.016/2.67

[a] Values in the parentheses are for the highest resolution shell.
[b] Values in the parentheses are for anomalous multiplicity.
[c] $R_{meas} = \{\sum_h \sqrt{\{n_h/n_h - 1\}} \sum_j |\hat{I}_h - \hat{I}_{hj}|\} / \sum_{hj} I_{hj}$ with $\hat{I}_{hj} = (\sum_j I_{hj})/n_h$ and where n_h is the multiplicity of h.
[d] $R_{cryst} = \sum_{hkl} ||F_o| - k|F_c|| / \sum_{hkl} F_o$, where F_o and F_c are observed and calculated structure factors, respectively. R_{free} is R_{cryst} calculated for a test set of randomly chosen 5% of the data.

group with "structural waters" W24 and W12, as no other DNA contacts less than 4 Å are made by the Y123 side chain. In a corresponding mutagenesis study of MBD1, reduced mCpG binding caused by loss of the hydroxyl group of Y34 (Y34F is equivalent to Y123F in MeCP2; see Figure 1) was explained by loss of a putative hydrogen bond between Y34 and the amino group of m5C (Ohki et al., 2001). Our structure fails to support the equivalent Y123-m5C interaction in MeCP2, and a more likely explanation in the light of our closely analogous MeCP2 structure is that hydrogen bonds to bridging structural water molecules have been lost (Figure 2E). Further evidence for the importance of this interaction comes from mutagenesis of mammalian MBD3, which does not normally bind specifically to methylated DNA and has phenylalanine (F34 in MBD3) in place of tyrosine at the equivalent position (see Figure 1). Interestingly, MBD3 can be converted into a methyl-CpG-binding protein by addition of a hydroxyl group via an F34Y mutation (Fraga et al., 2003). In addition to Y123, D121 is involved in water coordination, although this residue also forms a direct CH…O interaction with the methyl group of m5C8 (Figure 2E) and two hydrogen bonds to R111. Mutagenesis of this aspartate in MeCP2 (D121A or D121C; Free et al. [2001]) or the equivalent residue in MBD1 (D32A; Ohki et al. [2001]) severely reduces binding to methylated DNA. The mutagenesis data derived from several members of the MBD protein family therefore support the structural evidence that water is a key feature for recognition of mCpG by MBD domains.

We propose that the water-mediated recognition mode established here is conserved in other members of the MBD protein family. The crystal structure of the MeCP2 MBD complexed with DNA indeed resembles the NMR structure of the MBD1 MBD-DNA complex published by Ohki and coworkers (Ohki et al., 2001) with an rmsd fit of C_α atoms of 4.2 Å (Figure S2). It was previously deduced, however, that recognition of the cytosine methyl groups by MBD1 depends upon a hydrophobic patch comprising five amino acids that are conserved among MBD proteins (Ohki et al., 2001). Water molecules were not considered in the MBD1 structure, and it is possible that analysis of spin diffusion effects mediated by tightly bound waters will permit reconciliation of the NMR data with the hydrogen bond configuration reported here.

The C-terminal region of the MBD comprises an unusual tandem "Asx-ST motif" (Figure 4) that consists of an Asx turn (^{156}DFT^{158}) followed immediately by an ST motif (Wan and Milner-White, 1999a, 1999b) (^{158}TVTG^{161}). The Asx turn is formed by a hydrogen bond that connects the main-chain NH group of T158 and the side-chain carbonyl of D156. The ST motif is held together by hydrogen bonds to the hydroxyl group of T158 (Figure 4). The tandem motif is further stabilized by hydrogen bonds to R106 via the main-chain carbonyl group of T158 and V159 (Figure 4). The structure shows that T158 occupies a pivotal position that coordinates the two consecutive turns. To test this, we assayed the effect of T158 mutations on DNA binding. T158M, which is the most common missense mutation causing RTT, abolished DNA binding under our experimental conditions (Figure 3). Substitution of T158 by the smaller alanine side chain (T158A; also a RTT mutation) again strongly impaired DNA binding, arguing against a purely steric interference by the bulky methionine side chain. In contrast, T158S, which retains the hydroxyl group that is implicated in hydrogen bond stabilization of the tandem Asx-ST motif, maintained substantial affinity for methylated DNA (Figure 3).

It is notable that two of the four most frequent missense mutations found in RTT (T158M and R106W [Figure 1, databases at http://www.mecp2.org.uk and http://mecp2.chw.edu.au]) affect residues that stabilize the tandem Asx-ST motif. The structure is not induced by DNA binding, as it is present in the unliganded MeCP2 MBD (see Figure 2C) (Wakefield et al., 1999). The Asx-ST motif contacts DNA via a hydrogen bond between V159(N) of the Asx-ST motif and the phosphate oxygen of T31 (base paired with A11) at the start of the AT run (^{11}AATT^{14}) (Figure 4 and Table S2). Runs of four to six consecutive A/T bases are known to cause narrowing of the minor groove, leading to DNA bending (Figure S3A). In our structure, interphosphate distances showed a minor groove at ^{11}AATT^{14} that is significantly (2.9 Å) narrower than an ideal B-DNA minor groove (Figure S3B). We speculate that the DNA bend due to the ^{11}AATT^{14} run is required to accommodate the stabilizing interaction with the Asx-ST motif in intact MeCP2.

The locations of naturally occurring *MECP2* mutations that underlie RTT and other neurological conditions highlight the importance of the MBD domain (Amir et al., 1999; Bienvenu and Chelly, 2006; Kriaucionis and Bird, 2003). More than half of all

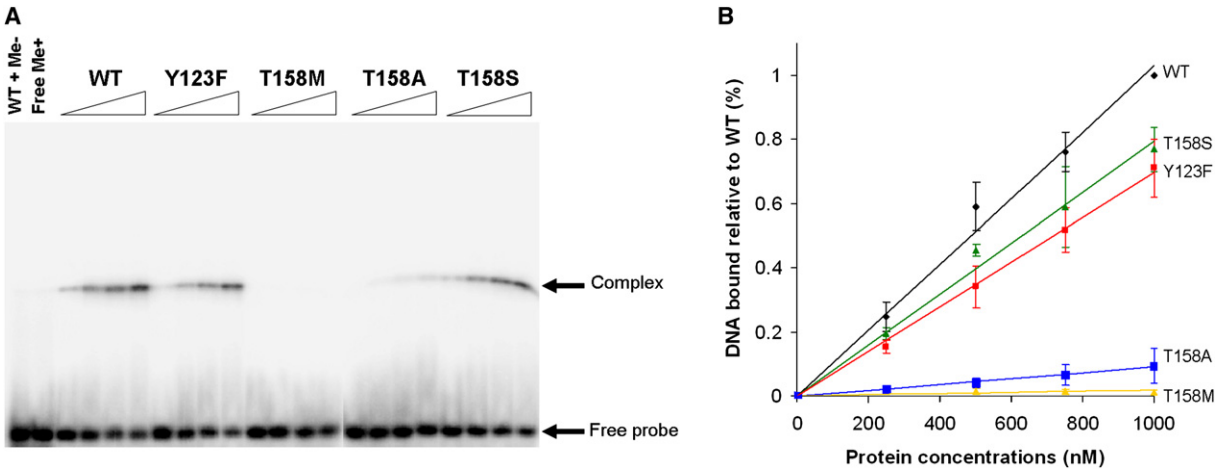

Figure 3. Mutagenesis Confirms the Importance of Y123 and T158 for MBD Binding to Methylated DNA In Vitro

(A) Electrophoretic mobility shift assays were performed with the 20 bp *BDNF* DNA sequence as probe in the presence of wild-type (WT) or mutant forms of the 77–167 fragment of MeCP2. The first lane (WT+Me−) shows absence of a protein DNA complex between wild-type MBD and nonmethylated DNA. Binding to methylated DNA is disrupted by T158M and T158A mutations, whereas binding is minimally affected by the conservative T158S mutation. The Y123F mutation significantly reduces DNA binding.

(B) A plot of the fraction of labeled probe complexed at protein concentrations of 250 nM, 500 nM, 750 nM, and 1 μM as measured by densitometry. Estimated standard deviations (shown as vertical bars) were calculated from measured intensities from three separate gels and scaled to the band from the probe complexed with 1 μM wild-type MBD, which was taken as 100%. Plots refer to WT (black), T158A (blue), T158M (yellow), T158S (green, from two measurements), and Y123F (red).

known disease-causing missense mutations affect the core MBD between amino acids 97 and 161, although this constitutes only ~13% of the total amino acid sequence. Complete conservation of the amino acid sequence of the MeCP2 MBD between mice and humans further emphasizes its functional significance.

The unexpected water-mediated recognition of the methylated CpG dinucleotide and the involvement of an unusual Asx-ST motif can account for the effects of a number of biologically important site point mutants in the MBD family. Future studies focusing on MeCP2 domains in complex with macromolecular

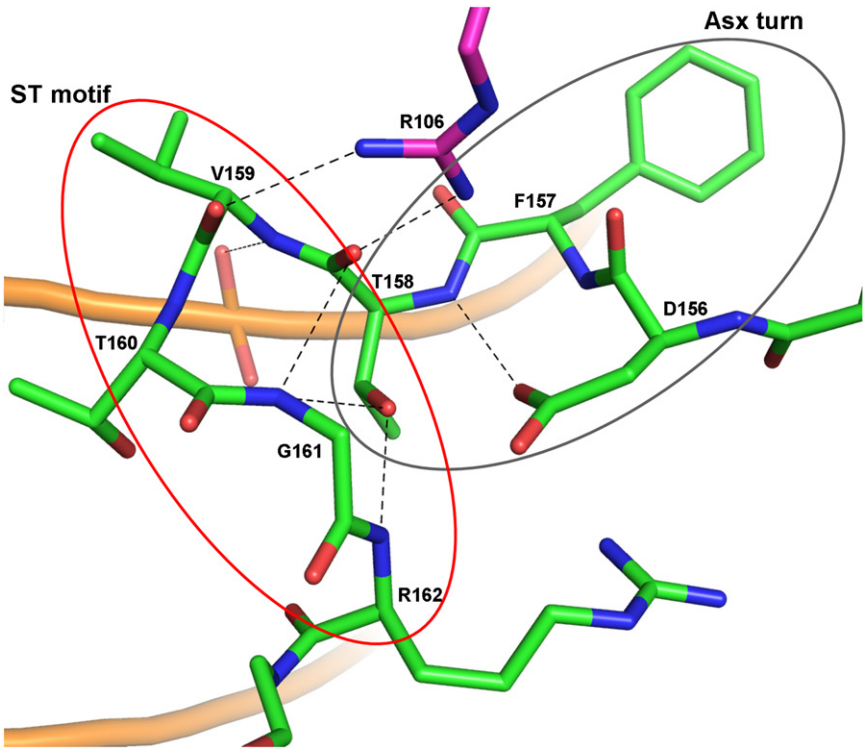

Figure 4. T158 Plays a Structurally Important Role in Forming the Tandem Asx-ST Motif

The Asx turn is composed of D156, F157, and T158, with the motif-defining hydrogen bond formed between the carboxylate side chain and the main-chain amine nitrogen of T158. The ST motif is the modified β turn consisting of T158, V159, T160, G161, and R162 with the side-chain hydroxyl group of T158 hydrogen bonding to the main-chain nitrogen atoms of G161 and R162.

partners promise to illuminate further the molecular role of this protein in interpreting the DNA-methylation signal.

EXPERIMENTAL PROCEDURES

Protein Expression and Purification

Recombinant proteins were expressed and purified as initially described (Klose and Bird, 2004) with some modifications. After cell recovery and sonication, bacterial crude lysate was loaded onto an Ni-NTA (Novagen) column on an FPLC system (Applied Biosystems) and washed with 12% N250 (20 mM NaH_2PO_4, 300 mM NaCl, 250 mM imidazole). Protein was eluted with a gradient from 12%–40% of N250. Peak fractions containing MBD were pooled, concentrated, and applied onto a Sephacryl-200 gel filtration column on an FPLC system. Fractions containing MBD protein were pooled and loaded onto a cation-exchange SP-Sepharose column. Peak fractions were eluted with a linear gradient of 300–500 mM NaCl, containing 20 mM HEPES (pH 7.9). Fractions were combined and dialyzed overnight into CE300 (20 mM HEPES [pH 7.6], 300 mM NaCl). Protein was concentrated to ~30 mg/ml and kept at 277K.

For the production of selenomethionyl protein, the recombinant plasmid was transformed into methionine-deficient B834(DE3)pLys cells. Cells were grown in minimal medium containing selenomethionine (10 mg/ml) and the other 19 amino acids (4 mg/ml each). Expression and purification of selenomethionyl protein was then performed as above except 1 mM of DTT was incorporated in all buffers.

Incorporation of Methionine by Site-Directed Mutagenesis

Site-directed mutagenesis was carried out according to the manufacturer's protocol (QuikChange, Stratagene). A pair of mutagenic primers was designed to contain the desired point mutation. Mutant plasmids were then transformed into BL21(DE3)pLys or B834(DE3)pLys cells for native or selenomethionyl mutant protein expression and purified as described above.

Nucleic Acid Preparation

Oligonucleotides for cocrystallization were synthesized by Oligos Etc. (Wilsonville, OR) and purified by HPLC. The lyophilized oligonucleotides were resuspended in TEN buffer (10 mM Tris-HCl [pH 8.0], 0.5 mM EDTA, 100 mM NaCl) to a concentration of 2 mM. Complementary strands were mixed in equimolar amounts and annealed by heating to 368K and then cooled to room temperature over 3 hr.

Crystallization

The complex of DNA-protein was prepared by mixing a 1:1.3 ratio of protein to DNA in CE100 (20 mM HEPES [pH 7.9], 100 mM NaCl) and incubated at room temperature for 30 min to promote complex formation. The final concentration of DNA and protein were 260 and 200 μM, respectively. Equal volumes of the DNA-protein complex and precipitant solution (26% PEG2000, 200 mM ammonium acetate, 10 mM Mg acetate, 50 mM Na cacodylate [pH 6.5], 2 mM DTT) were mixed and equilibrated against the precipitant solution using the hanging drop vapor diffusion method. Rectangular crystals with maximum dimension of 0.5 mm grew within 3 days. The crystals were flash frozen in liquid nitrogen. Most crystals diffracted to ~3 Å maximum resolution, but soaking the crystal for 15 min in a precipitant solution in which the Mg acetate was replaced with $MnCl_2$ (35% PEG2000, 200 mM ammonium acetate, 10 mM $MnCl_2$, 50 mM Na cacodylate [pH 6.5], 2 mM DTT) improved resolution to 2.5 Å.

Data Collection and Structural Determination

Native and anomalous data sets were collected at ESRF, Grenoble (Table 1). The structure was solved by SAD using the Se peak data set from the crystal, which was soaked in a solution containing 10 mM $MnCl_2$. These crystals belong to space group C2 with unit cell dimensions a = 79.71, b = 53.60, c = 65.73 Å, and β = 132.10°. There is one molecule per asymmetric unit with a calculated solvent content of 52.6%. Diffraction data were collected to a resolution of 2.5 Å (Table 1). MOSFLM/SCALA (CCP4, v6.0.1) (Potterton et al., 2002) was used to process the data, and the output was fed into PHENIX (Adams et al., 2002), which was used to locate the heavy atoms and for phase determination. Model building and refinement were performed with COOT (Emsley and Cowtan, 2004) and REFMAC5.2 (Murshudov et al., 1997), and the fully refined structure gave calculated R_{cryst} and R_{free} values of 21.2 and 27.6, respectively. Structural analysis was performed using MSDMotif server (Golovin et al., 2004), 3DNA (Lu and Olson, 2003), and HBPLUS (McDonald and Thornton, 1994). All figures were prepared using PyMOL (DeLano, 2003).

Gel Retardation Assay

All oligonucleotides for gel retardation assays were synthesized by Sigma-Genosys and purified by desalting. The protocol for ^{32}P-dATP labeling and native gel electrophoresis was described previously (Klose et al., 2005).

ACCESSION NUMBERS

The atomic coordinates of the MeCP2 MBD domain cocrystallized with a 20 bp DNA fragment have been deposited with the Protein Data Bank (PDB) under the accession code 3C2I.

SUPPLEMENTAL DATA

Supplemental Data include three figures, two tables, and Supplemental References and can be found with this article online at http://www.molecule.org/cgi/content/full/29/4/525/DC1/.

ACKNOWLEDGMENTS

This work was supported by the Wellcome Trust. K.L.H. is a Darwin Trust Postgraduate Student, I.W.M. is supported by Edinburgh Lead Discovery and a Wellcome Trust VIP Grant, L.S. is supported by the Deutsche Forschungsgemeinschaft, and R.J.K. was a Wellcome Trust Prize Student. Synchrotron data collection was supported by the European Synchrotron Radiation Facility, Grenoble, France. We thank Dr. J. Richardson and Professor J. Milner-White for helpful discussion.

Received: July 13, 2007
Revised: October 25, 2007
Accepted: December 15, 2007
Published: February 28, 2008

REFERENCES

Adams, P.D., Grosse-Kunstleve, R.W., Hung, L.W., Ioerger, T.R., McCoy, A.J., Moriarty, N.W., Read, R.J., Sacchettini, J.C., Sauter, N.K., and Terwilliger, T.C. (2002). PHENIX: building new software for automated crystallographic structure determination. Acta Crystallogr. D Biol. Crystallogr. *58*, 1948–1954.

Amir, R.E., Van den Veyver, I.B., Wan, M., Tran, C.Q., Francke, U., and Zoghbi, H.Y. (1999). Rett syndrome is caused by mutations in X-linked MECP2, encoding methyl-CpG-binding protein 2. Nat. Genet. *23*, 185–188.

Amir, R.E., Van den Veyver, I.B., Schultz, R., Malicki, D.M., Tran, C.Q., Dahle, E.J., Philippi, A., Timar, L., Percy, A.K., Motil, K.J., et al. (2000). Influence of mutation type and X chromosome inactivation on Rett syndrome phenotypes. Ann. Neurol. *47*, 670–679.

Ballestar, E., Yusufzai, T.M., and Wolffe, A.P. (2000). Effects of Rett syndrome mutations of the methyl-CpG binding domain of the transcriptional repressor MeCP2 on selectivity for association with methylated DNA. Biochemistry *39*, 7100–7106.

Berman, H.M., Olson, W.K., Beveridge, D.L., Westbrook, J., Gelbin, A., Demeny, T., Hsieh, S.H., Srinivasan, A.R., and Schneider, B. (1992). The nucleic acid database. A comprehensive relational database of three-dimensional structures of nucleic acids. Biophys. J. *63*, 751–759.

Bienvenu, T., and Chelly, J. (2006). Molecular genetics of Rett syndrome: when DNA methylation goes unrecognized. Nat. Rev. Genet. *7*, 415–426.

Bird, A. (2002). DNA methylation patterns and epigenetic memory. Genes Dev. *16*, 6–21.

Chen, W.G., Chang, Q., Lin, Y., Meissner, A., West, A.E., Griffith, E.C., Jaenisch, R., and Greenberg, M.E. (2003). Derepression of BDNF transcription involves calcium-dependent phosphorylation of MeCP2. Science *302*, 885–889.

Couture, J.F., Hauk, G., Thompson, M.J., Blackburn, G.M., and Trievel, R.C. (2006). Catalytic roles for carbon-oxygen hydrogen bonding in SET domain lysine methyltransferases. J. Biol. Chem. *281*, 19280–19287.

DeLano, W.L. (2003). The PyMOL molecular graphics system (San Carlos, CA: DeLano Scientific).

Emsley, P., and Cowtan, K. (2004). Coot: model-building tools for molecular graphics. Acta Crystallogr. D Biol. Crystallogr. *60*, 2126–2132.

Fraga, M.F., Ballestar, E., Montoya, G., Taysavang, P., Wade, P.A., and Esteller, M. (2003). The affinity of different MBD proteins for a specific methylated locus depends on their intrinsic binding properties. Nucleic Acids Res. *31*, 1765–1774.

Free, A., Wakefield, R.I., Smith, B.O., Dryden, D.T., Barlow, P.N., and Bird, A.P. (2001). DNA recognition by the methyl-CpG binding domain of MeCP2. J. Biol. Chem. *276*, 3353–3360.

Golovin, A., Oldfield, T.J., Tate, J.G., Velankar, S., Barton, G.J., Boutselakis, H., Dimitropoulos, D., Fillon, J., Hussain, A., Ionides, J.M., et al. (2004). E-MSD: an integrated data resource for bioinformatics. Nucleic Acids Res. *32*, D211–D216.

Guy, J., Gan, J., Selfridge, J., Cobb, S., and Bird, A. (2007). Reversal of neurological defects in a mouse model of Rett syndrome. Science *315*, 1143–1147.

Hendrich, B., and Bird, A. (1998). Identification and characterization of a family of mammalian methyl-CpG binding proteins. Mol. Cell. Biol. *18*, 6538–6547.

Jones, P.L., Veenstra, G.J.C., Wade, P.A., Vermaak, D., Kass, S.U., Landsberger, N., Strouboulis, J., and Wolffe, A.P. (1998). Methylated DNA and MeCP2 recruit histone deacetylase to repress transcription. Nat. Genet. *19*, 187–191.

Klose, R.J., and Bird, A.P. (2004). MeCP2 behaves as an elongated monomer that does not stably associate with the Sin3a chromatin remodeling complex. J. Biol. Chem. *279*, 46490–46496.

Klose, R.J., Sarraf, S.A., Schmiedeberg, L., McDermott, S.M., Stancheva, I., and Bird, A.P. (2005). DNA binding selectivity of MeCP2 due to a requirement for A/T sequences adjacent to methyl-CpG. Mol. Cell *19*, 667–678.

Kriaucionis, S., and Bird, A. (2003). DNA methylation and Rett syndrome. Hum. Mol. Genet. *12*(Spec 2), R221–R227.

Kudo, S., Nomura, Y., Segawa, M., Fujita, N., Nakao, M., Dragich, J., Schanen, C., and Tamura, M. (2001). Functional analyses of MeCP2 mutations associated with Rett syndrome using transient expression systems. Brain Dev. *23* (*Suppl 1*), S165–S173.

Lu, X.J., and Olson, W.K. (2003). 3DNA: a software package for the analysis, rebuilding and visualization of three-dimensional nucleic acid structures. Nucleic Acids Res. *31*, 5108–5121.

Luscombe, N.M., Laskowski, R.A., and Thornton, J.M. (2001). Amino acid-base interactions: a three-dimensional analysis of protein-DNA interactions at an atomic level. Nucleic Acids Res. *29*, 2860–2874.

Martinowich, K., Hattori, D., Wu, H., Fouse, S., He, F., Hu, Y., Fan, G., and Sun, Y.E. (2003). DNA methylation-related chromatin remodeling in activity-dependent BDNF gene regulation. Science *302*, 890–893.

Mayer-Jung, C., Moras, D., and Timsit, Y. (1998). Hydration and recognition of methylated CpG steps in DNA. EMBO J. *17*, 2709–2718.

McDonald, I.K., and Thornton, J.M. (1994). Satisfying hydrogen bonding potential in proteins. J. Mol. Biol. *238*, 777–793.

Murshudov, G.N., Vagin, A.A., and Dodson, E.J. (1997). Refinement of macromolecular structures by the maximum-likelihood method. Acta Crystallogr. D Biol. Crystallogr. *53*, 240–255.

Nan, X., Meehan, R.R., and Bird, A. (1993). Dissection of the methyl-CpG binding domain from the chromosomal protein MeCP2. Nucleic Acids Res. *21*, 4886–4892.

Nan, X., Campoy, J., and Bird, A. (1997). MeCP2 is a transcriptional repressor with abundant binding sites in genomic chromatin. Cell *88*, 471–481.

Nan, X., Ng, H.-H., Johnson, C.A., Laherty, C.D., Turner, B.M., Eisenman, R.N., and Bird, A. (1998). Transcriptional repression by the methyl-CpG-binding protein MeCP2 involves a histone deacetylase complex. Nature *393*, 386–389.

Neul, J.L., and Zoghbi, H.Y. (2004). Rett syndrome: a prototypical neurodevelopmental disorder. Neuroscientist *10*, 118–128.

Ohki, I., Shimotake, N., Fujita, N., Nakao, M., and Shirakawa, M. (1999). Solution structure of the methyl-CpG-binding domain of the methylation-dependent transcriptional repressor MBD1. EMBO J. *18*, 6653–6661.

Ohki, I., Shimotake, N., Fujita, N., Jee, J., Ikegami, T., Nakao, M., and Shirakawa, M. (2001). Solution structure of the methyl-CpG binding domain of human MBD1 in complex with methylated DNA. Cell *105*, 487–497.

Potterton, E., McNicholas, S., Krissinel, E., Cowtan, K., and Noble, M. (2002). The CCP4 molecular-graphics project. Acta Crystallogr. D Biol. Crystallogr. *58*, 1955–1957.

Wakefield, R.I., Smith, B.O., Nan, X., Free, A., Soteriou, A., Uhrin, D., Bird, A.P., and Barlow, P.N. (1999). The solution structure of the domain from MeCP2 that binds to methylated DNA. J. Mol. Biol. *291*, 1055–1065.

Wan, W.Y., and Milner-White, E.J. (1999a). A natural grouping of motifs with an aspartate or asparagine residue forming two hydrogen bonds to residues ahead in sequence: their occurrence at α-helical N termini and in other situations. J. Mol. Biol. *286*, 1633–1649.

Wan, W.Y., and Milner-White, E.J. (1999b). A recurring two-hydrogen-bond motif incorporating a serine or threonine residue is found both at α-helical N termini and in other situations. J. Mol. Biol. *286*, 1651–1662.